PERGAMON

International Journal of Heat and Mass Transfer 41 (1998) 4327–4340

International Journal of HEAT and MASS TRANSFER

# Onset of transition to turbulence in natural convection with gas along a vertical isotherm plane

Marcel Jannot, Thierry Kunc*

*BERTIN Society and Co., B.P. No. 3, 78373 Plaisir cedex, France*

Received 11 December 1995; in final form 15 January 1998

**Abstract**

It is generally accepted that the onset of transition to the turbulence in free convection along a vertical isotherm plane with gas occurs at a given Grashof number. A more subtle reality became apparent thirty years ago in the course of experiments carried out with either small installations and pressurized gas or under atmospheric pressure with an experimental installation of great height. To elucidate the problem, a re-examination of data set and a new analysis have been made. This has led to a physical interpretation of what was observed : the origin of the instability which is triggered off in this boundary layer lies in interaction between the zone beyond this boundary layer where there is a vertical stratification of temperature and the boundary layer near the plane. This is based on the comparison between characteristic times calculated for the two zones in question. 

**Nomenclature**

$C_p$ specific heat at constant pressure [J kg$^{-1}$ K$^{-1}$]
$C_v$ specific heat at constant volume [J kg$^{-1}$ K$^{-1}$]
$Ec$ Eckert number
$f$ frequency [Hz]
$Fr$ Froude number
$g$ gravitational acceleration [m s$^{-2}$]
$Gr$ Grashof number
$h$ heat transfer coefficient [W m$^{-2}$ K$^{-1}$]
$H$ height [m]
$k$ thermal conductivity [W m$^{-1}$ K$^{-1}$]
$K_1$, $K_2$, $K_3$, $K_4$, $k_1$, $k_2$, $k_3$ dimensionless constants
$L$ length [m]
$N$ dimensionless number ($Fr \times Ec$)
$N_p$, $N_x$, $N_{\Delta T}$ dimensionless numbers relative, respectively, to $P$, $x$ and $(T_w - T_\infty)$
$O(A)$ same proportion as $A$
$P$ pressure [N m$^{-2}$]
$Pr$ Prandtl number
rot rotational operator [m$^{-1}$]
$t$ time [s]
$t_B$ boundary layer oscillation time [s]
$t_{osc}$ oscillator time (period) [s]
$t_v$ transversal viscous communication time [s]
$T$ absolute temperature [K]
$T_w$ wall temperature [K]
$T_\infty$ temperature outside the boundary layer [K]
$u$, $v$ velocity components in the $x$, $y$ system of co-ordinates [m s$^{-1}$]
$U$, $V$ velocity [m s$^{-1}$]
$W$ width [m]
$x$, $y$ Cartesian co-ordinates [m].

*Greek symbols*

$\beta$ thermal expansion coefficient [K$^{-1}$]
$\delta$ boundary layer thickness [m]
$\delta u$, $\delta v$, $\delta \rho$, $\delta T$, $\delta P$ disturbance of $u$, $v$, $\rho$, $T$, $P$, respectively
$\Delta$ $\nabla^2$ [m$^{-2}$]
$\zeta$ vorticity component [s$^{-1}$]
$\lambda$ wavelength [m]
$\mu$ dynamic viscosity [kg m$^{-1}$ s$^{-1}$]
$\nu$ cinematic viscosity [m$^2$ s$^{-1}$]
$\rho$ density [kg m$^{-3}$]
$\phi_\mu$ viscous dissipation function [kg m$^{-1}$ s$^{-3}$]
$\nabla$ Nabla operator [m$^{-1}$].

*Subscripts*

at atmospheric pressure conditions
av average
BV Brunt–Väisälä

* Corresponding author.

0017–9310/98 $19.00 
PII : S0017–9310(98)00068–4

H high
L low
max maximum
tr transition
w wall
$\infty$ outer boundary layer.

*Superscripts*
$\bar{}$ steady state
$\cdot$ time derivation.

## 1. Introduction

Previous publications [1–5], gave a set of experimental results on natural convection including laminar–turbulent transition in free convection along a vertical isothermal plane. This research was undertaken under contract with Electricité De France and Euratom in order to solve thermal insulation problems for pressurized gas nuclear reactors.

In a preliminary report in 1963, Mordchelles-Regnier and Kaplan [1], described what we had observed originally: "The conditions for transition to the turbulent regime on a single vertical plate depend not only on the Grashof number but also on the height at which the turbulence appears". Thirty years on, many excellent textbooks in the field of convection, heat and mass transfer (e.g. [6] p. 268 in the 1995 edition) still give a constant Grashof number as a condition for turbulent transition. This is because in free convection the Grashof number plays a role similar to that played by the Reynolds number in forced convection. During the laminar–turbulent transition the role played by these two numbers can be clarified by taking the ratio $t_v/t_B$, where $t_v$ and $t_B$ are two characteristic time scales:

—$t_v$ characterises the transversal viscous communication time;
—$t_B$ characterises the eddy formation time (or period for travelling waves in the boundary layer).

As already stated above, the problem is that in free convection a constant Grashof number for transition is in contradiction with the observations made during experiments. A more extensive analysis is therefore necessary. There are currently many textbooks on the subject of transition (e.g. [6–9]), chaos and non-linear dynamic systems (e.g. [10, 11]). Various analyses are to be found in these books on the simplified meteorological model by Lorentz [12], and on the Rayleigh–Benard instability, but seldom or with only a passing reference to vertical plane configurations. However, there are some exceptions which deal with the present subject: Dring and Gebhart [13] have presented an analytical study with a numerical solution for laminar natural convection boundary layer flow over a vertical surface with uniform heat flux. Godaux and Gebhart [14] have observed transition in a experimental study of natural convection flow adjacent to a vertical surface. Gebhart and Mahajan [15] have compared prediction and experiments about characteristic disturbance frequency in vertical natural convection flow. More recently, Bejan and Cunnington [16] have developed a theoretical model of turbulent transition in natural convection near a vertical wall using an inviscid jet model. Due note has been taken of all these articles, in particular of the fact that instability can arise from the coupling of two oscillators ([11] p. 273). In the present case interaction is possible between the boundary layer which spreads along the plane and the fluid which remains stationary beyond the boundary layer. In this area, viscous effects are negligible, the fluid reacting like an inviscid fluid and there is a vertical temperature stratification. Väisälä [17] in 1925, Brunt [18] in 1927, then Glansdorff and Prigogine [9] p. 178 in 1971, demonstrated in the case of geophysical applications, that under these conditions an oscillation of part of the fluid is possible. The frequency of this oscillation is called Brunt–Väisälä frequency ($f_{BV}$). The associated period $t_{osc} = 1/f_{BV}$ is a new time scale to compare with the early one, giving a new criterion for the laminar–turbulent transition.

Usually, Brunt–Väisälä frequency is connected to a notion of internal gravity waves in fluid within boundaries. In this case, stationary waves depend on $f_{BV}$ and on boundary measurements (e.g. Thorpe [19] where $f_{BV}$ appears but is not identified as such). There are many geophysical applications where the $f_{BV}$ is present. Benielli and Sommeria [20, 21], treat the case of stratified fluid in interaction with a vertical boundary layer. According to Ndame and Penot [22, 23] then Xin and Le Quéré [24], the influence of $f_{BV}$ in natural convection was first envisaged by Patterson and Imberger [25] in 1980. Ndame [22] p. 40, Xin and Le Quéré [24] p. 106, think that this frequency does not explain the onset of transition to turbulence. Their argumentation is that the internal wave notions are dispersive but only slightly dissipative, and located mainly in the core of the cells where only one very small frequency would be activated contrary to the band of small frequency observed.

Le Quéré, Xin, Henkes [24, 26–28], treat the transition to turbulence in rectangular cells by numerical simulation.

This paper is set out following different stages:

—synthesis of various experimental works, examination and presentation.
—Grashof transition number evaluation in analogy with forced convection. There would appear to be several orders of magnitude between evaluation and measurements.
—new assessment by a more direct way of the Brunt–

Väisälä frequency ($f_{BV}$) evaluation. In addition it is shown that a pendular mode with the same frequency is also possible.

—assessment of the ratios $t_v/t_B$ and $t_{osc}/t_B$, where $t_{osc} = 1/f_{BV}$.

—comparison with measurements which show that a new physical interpretation is possible in accordance with the measurements if taken in consideration of the fact that the vertical gradient of temperature outside the boundary layer evolves with the plane temperature.

## 2. Observations made during the experiments

The first stage for transition from laminar to turbulent flow is the boundary layer oscillations with a wavelength in relation to the boundary layer thickness. Such oscillations are always present from time to time (that is one of the reasons for the intermittence phenomenon) because of small disturbances coming from the outer flow. A predominantly periodic phenomenon can be observed during the transition onset. Sometimes the oscillations are dampened but more often the wave becomes irregular in shape and ends up by breaking down, transforming into vortices and finally fragmenting into the smaller scaled turbulence. These oscillations are basically of the same nature as the waves which can be observed in forced convection along a flat surface. The researcher's task is rendered more difficult by virtue of the intermittence of this phenomenon for he has to locate the exact place where instabilities begin. The transition was detected by differential interferometry except for [4] where it was detected by heat fluxmeters placed on the plane (see Table 1 in the Appendix).

Figure 1 illustrates the onset of the transition which takes place along a plane wall situated in ambient air. Note the stretching and the folding of the boundary layer.

The presentation of results in [2] and [3] was (Fig. 2):

$$g\frac{\beta x}{C_p} = 0.546\cdot 10^{13}\left[\left(\frac{C_p}{\beta}\right)^{3/2}\frac{1}{gv}\right]^{-3/2}\frac{1}{\beta(T_w - T_\infty)}.$$

This form was retained because for measurements: $N_x = g(\beta x/C_p) = Cte\cdot x$; $N_p = (C_p/\beta)^{3/2}(1/gv) = Cte\cdot P$; $N_{\Delta T} = \beta(T_w - T_\infty) = Cte\cdot(T_w - T_\infty)$ are dimensionless parameters which characterise, respectively, $x$, $P$ and $(T_w - T_\infty)$.

The experimental correlation can also be written thus:

$$Gr_x = 0.96\cdot 10^{17}[N_{\Delta T}^{-0.4}\cdot N_x^2]^{5/6}.$$

As $N_x = [g(\beta/C_p)]x$, where $g(\beta/C_p)$ is almost constant for all measurements, then $N_x = x/L$, where $L$ should be a length to be determined, but remaining constant for each configuration.

A new presentation of the data is given in Fig. 3.

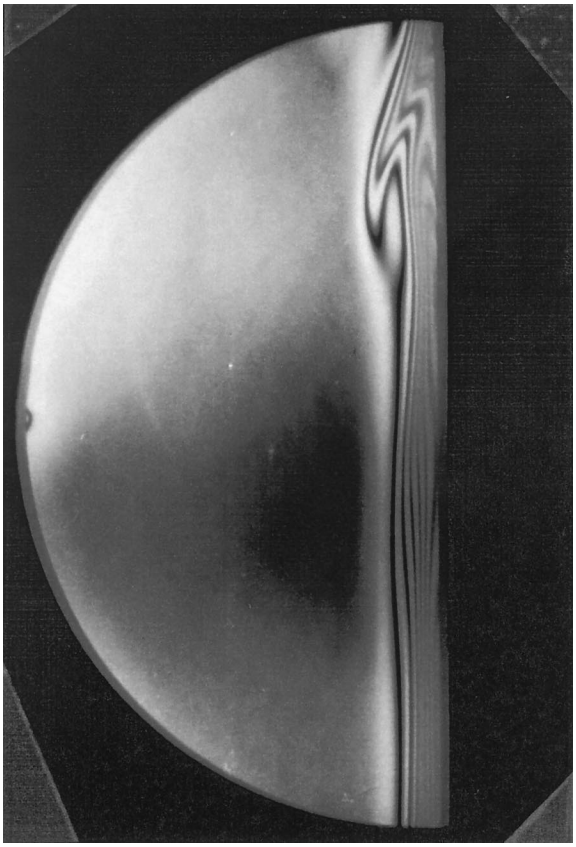

Fig. 1. Transition visualization.

For these experiments, pressurized gas was used from 1 to 30 bars and several sizes of plane, or at the atmospheric pressure with two sizes of plane, one of which was 3.2 m high. It was easier in these conditions to explore a wide field of parameters where the transition occurs than in experiments with a single configuration. In [5], a dimensional analysis was used to suggest a data correlation. This led to the use of the following number: $N = [gL/(C_p(T_w - T_\infty)]$, equivalent to $(gL/U^2)[U^2/(C_p(T_w - T_\infty)]$, i.e., the product of the Froude number by the Eckert number in order to interpret the experimental data. This parameter, which is always small, is introduced by the compressibility pressure stress work in energy equation where, although of the first order, it is to be compared to the vertical gradient of temperature. It can therefore seem suspect (except when the vertical gradient of temperature tends to zero) to give a physical justification of such measurements with this parameter because for gas, $g/C_p$ is almost always constant and is generally very small compared with the vertical temperature gradient.

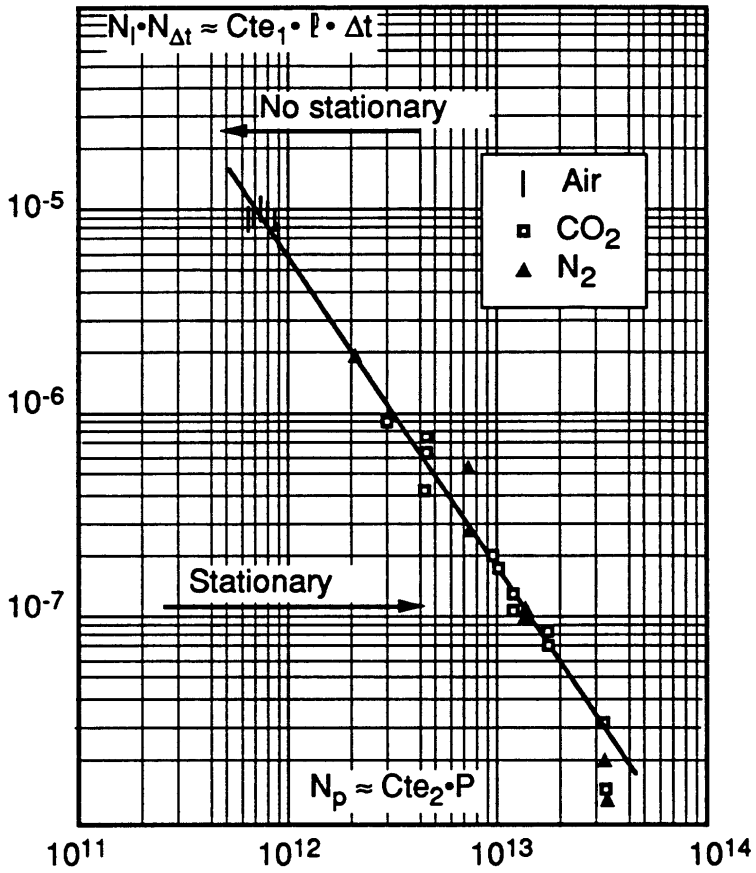


Fig. 2. Previous presentation of measurements from [2–4].

## 3. Examination of hypothesis: laminar–turbulent transition in free convection occurs in conditions similar to those for forced convection

Figure 4 illustrates how the comparaison is made to evaluate the $Gr_x$ number. $U_{max}$ and $\delta$ have been taken in free convection as shown in ref. [29] p. 311.

The effect of the thermal stratification has not been considered in this evaluation, but it is known (see [6] p. 181) that is modifies only slightly the shape of the stationary boundary layer.

$$Re_x = \rho \frac{U_{max} x}{\mu} \approx 0.766 \left(\frac{20}{21} + Pr\right)^{-1/2} Gr_x^{1/2} = K_1 Gr_x^{1/2}$$

$$\frac{\delta}{x} \approx 3.93 \left(\frac{20}{21} + Pr\right)^{1/4} Pr^{-1/2} Gr_x^{1/4} = K_2 Gr_x^{-1/4}$$

therefore, $Re_{\delta_{tr/3}} = \frac{1}{3} Re_{x_{tr}} \cdot (\delta_{tr}/x) = (K_1 K_2/3) Gr_{x_{tr}}^{1/4}$. Then with $Pr = 0.72$, $Re_{\delta_{tr/3}} = 1.040 Gr_{x_{tr}}^{1/4}$

In forced convection the transition appears for:

$$Re_{x_{tr}} = \frac{\rho U x}{\mu} = K_3 \cdot 10^5 \quad \text{where } K_3 \approx 5$$

$$\frac{\delta}{x} \approx \frac{K_4}{\sqrt{Re_x}} \quad \text{where } K_4 = 4.64$$

i.e. $Re_{\delta_{tr}} = K_3^{1/2} K_4$.

By identification of the Reynolds transition number, based on the friction layer to take into account the universality of the transition phenomenon along the boundary layer, then finally:

$$Gr_{x_{tr}} = \left[\frac{3 K_3^{1/2} K_4}{K_1 K_2}\right]^4 \cdot 10^{10} = 10^{14}.$$

Figure 4 indicates how to evaluate comparative conditions during the transition between forced and free convection along a flat surface.

The Grashof transition number is shown in Fig. 3. It is of several orders of magnitude superior to the observations made. Another explanation must, therefore, be found.

## 4. Towards a physical interpretation

It is easy to justify why there is a vertical gradient of temperature in the experimental chamber. Except when

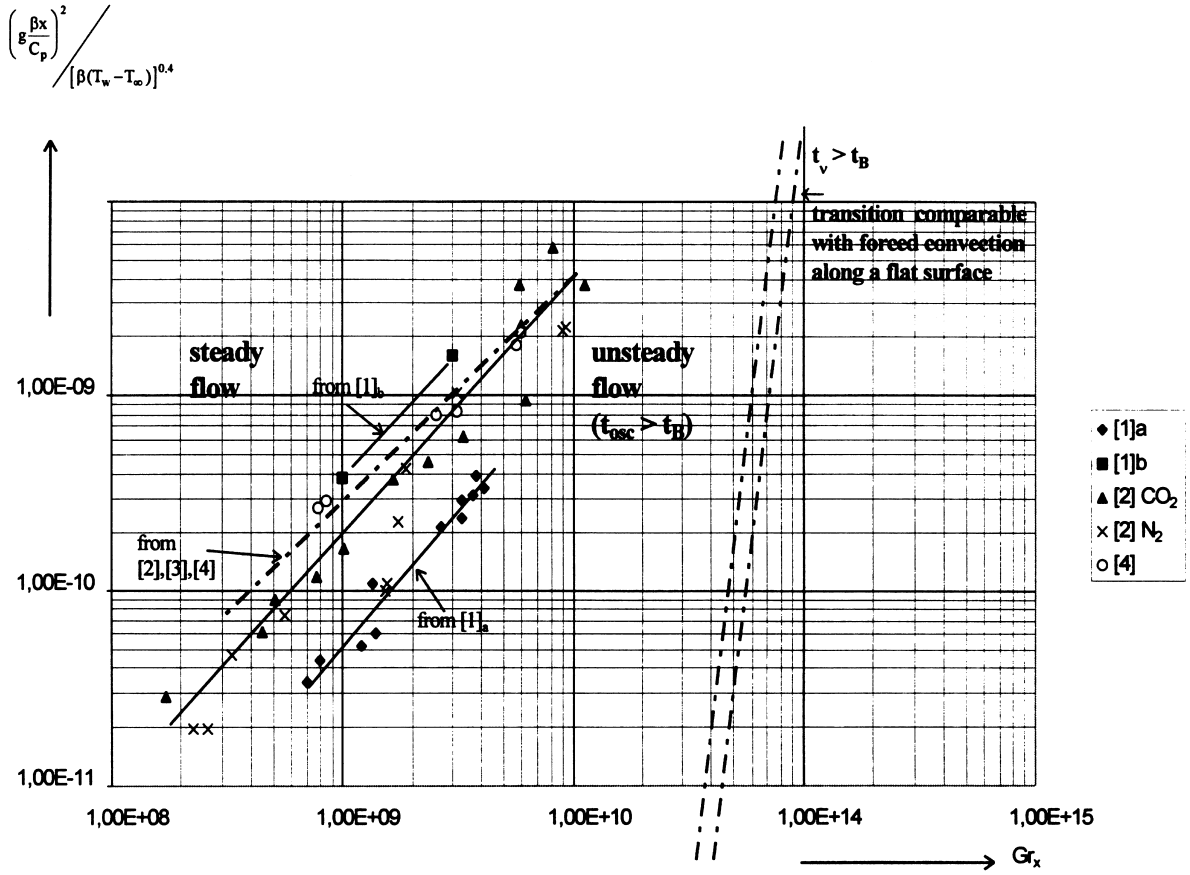


Fig. 3. Experimental conditions for transition in free convection along a vertical and isothermal plane (note the influence of the configuration). ■ data from $[1]_b$ air in ambient conditions. ◆ data from $[1]_a$ $CO_2$ in pressurized vessel of small height. ○ data from [4] air in ambient conditions and plane of great height. ▲ data from [2] $CO_2$ in pressurized vessel of medium height. × data from [2] $N_2$ in pressurized vessel of medium height.

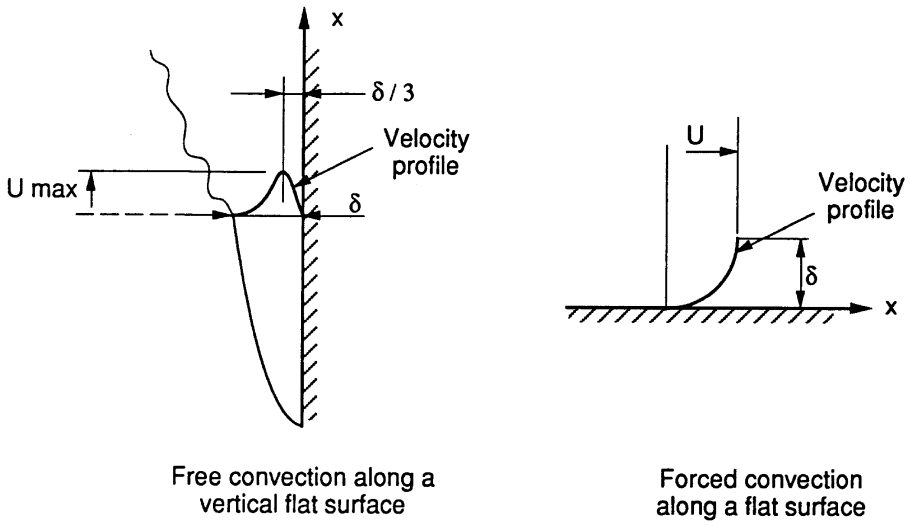


Fig. 4. Comparable transition for forced and free convection along a flat surface.

there is underfloor heating, the area outside the boundary layer is stratified with a positive gradient of temperature. This is because hot fluid rises and cold fluid descends.

See Fig. 5 for the schematization used to estimate the vertical gradient of temperature outside the boundary layer. It leads to:

$$\left.\frac{\partial T}{\partial x}\right|_{\infty} = \frac{(T_H - T_L)}{L} \gg \frac{g}{C_p}.$$

The length $L$ can be of same height as that of the plane or that of the height where the experimental plane is located, or a length to be defined.

### 4.1. General equations for the problem

Taking a gas with constant physical properties $(k, \mu, C_p)$ the equations used can be written as: momentum conservation

$$\rho\frac{\partial \mathbf{V}}{\partial t} + \rho(\mathbf{V}\cdot\nabla)\mathbf{V} = -\nabla P + \mu\nabla^2\mathbf{V} + \rho\mathbf{F}$$

mass conservation

$$\frac{\partial \rho}{\partial t} + \nabla\cdot(\rho\mathbf{V}) = 0 \tag{1}$$

energy conservation

$$\rho C_p\left(\frac{\partial T}{\partial t} + \mathbf{V}\cdot\nabla T\right) = k\nabla^2 T + \frac{\partial P}{\partial t} + \mathbf{V}\cdot\nabla P + \phi_\mu$$

fluid state

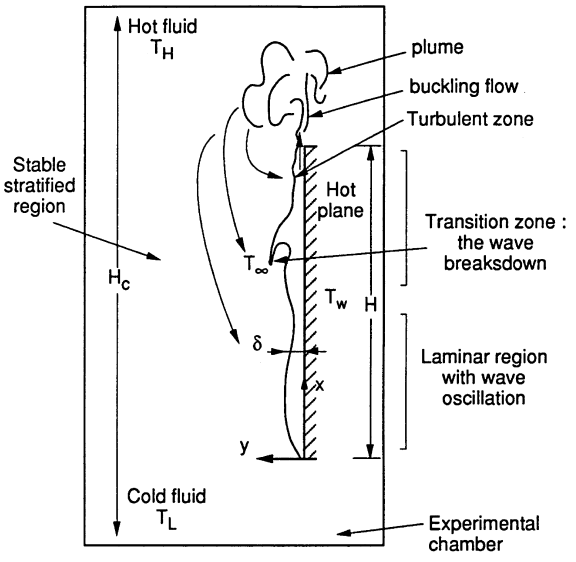


Fig. 5. Vertical gradient of temperature outside the boundary layer: $\partial T/\partial x|_\infty = [(T_H - T_L)/L] \gg (g/C_p)$. The length $L$ can be the same as that of the height $H_c$ of the chamber where the experimental plane is located near the wall or the same as the height $H$ of the wall, or another to be defined.

$$\frac{P}{\rho} = (C_p - C_v)T.$$

Taking the stability of the fluid outside the boundary layer; this problem was first analysed by Väisälä [15], Brunt [16] and then by Glansdorff and Prigogine in [9] p. 178. The result can be obtained direct from the equations (1). For the stationary state, the pressure and temperature profiles are linear:

$$\bar{u} = 0; \quad \bar{v} = 0; \quad \bar{T} = T_0 + \left.\frac{\partial \bar{T}}{\partial x}\right|_{\infty}\cdot x$$

$$\bar{P} \approx P_0 - \rho_0 g x; \quad \left.\frac{\partial \bar{T}}{\partial x}\right|_{\infty} = Cte$$

with perturbations:

$$u = \bar{u} + \delta u = \delta u$$

$$v = \bar{v} + \delta v = \delta v$$

$$T = \bar{T} + \delta T = T_0 + \left.\frac{\partial \bar{T}}{\partial x}\right|_{\infty} x + \delta T$$

$$P = \bar{P} + \delta P = P_0 - \rho_0 g x + \delta P.$$

Supposing now a brief perturbation for which viscous dissipation and thermal diffusion did not have enough time to take effect, the equations (1) then give for a first order approximation:

$$\frac{\partial \delta u}{\partial t} = g\beta\delta T - \frac{1}{\rho_0}\frac{\partial \delta P}{\partial x}$$

$$\frac{\partial \delta v}{\partial y} = -\frac{1}{\rho_0}\frac{\partial \delta P}{\partial y}$$

$$\frac{\partial \delta T}{\partial t} + \delta u\left(\left.\frac{\partial \bar{T}}{\partial x}\right|_{\infty} + \frac{g}{C_p}\right) = \frac{1}{\rho_0 C_p}\frac{\partial \delta P}{\partial t}. \tag{2}$$

Simplification is possible by assuming: $(1/\rho_0)(\partial\delta P/\partial x) \ll g\beta\delta T$ and $(1/\rho_0 C_p)(\partial\delta P/\partial t) \ll (\partial\delta T/\partial t)$, $\delta u$ and $\delta T$ dependent on only the temporal variable $t$, then:

$$\delta\dot{u} = g\beta\delta T$$

$$\delta\dot{T} = -\delta u\left(\left.\frac{\partial \bar{T}}{\partial x}\right|_{\infty} + \frac{g}{C_p}\right)$$

and by elimination of one variable:

$$\boxed{\begin{aligned} &\delta\ddot{u} + g\beta\left(\left.\frac{\partial \bar{T}}{\partial x}\right|_{\infty} + \frac{g}{C_p}\right)\delta u = 0 \\ &\delta\ddot{T} + g\beta\left(\left.\frac{\partial \bar{T}}{\partial x}\right|_{\infty} + \frac{g}{C_p}\right)\delta T = 0 \end{aligned}} \tag{3a}$$

these are the equations for a linear harmonic oscillator with the frequency:

$$f = \frac{1}{2\pi}\sqrt{g\beta\left(\left.\frac{\partial \bar{T}}{\partial x}\right|_{\infty} + \frac{g}{C_p}\right)} \tag{4}$$

i.e., the Brunt–Väisälä frequency.

Consequently a stable oscillator is possible only when:

$$\frac{x}{(T_w-T_\infty)}\left.\frac{\partial \bar{T}}{\partial x}\right|_\infty > \frac{xg}{(T_w-T_\infty)\cdot C_p} = \left(\frac{gx}{U^2}\right)\left(\frac{U^2}{(T_w-T_\infty)\cdot C_p}\right) = Fr\cdot Ec. \quad (5)$$

Applying the rotational operator to the momentum equation (1), a result similar to the previous one can be obtained (note rot · grad = 0):

$$\zeta = \frac{\partial \delta u}{\partial y} - \frac{\partial \delta v}{\partial x} \approx \frac{\partial \delta u}{\partial y}$$

(orthogonal component of the vorticity)

$$\frac{\partial \zeta}{\partial t} + \underbrace{\delta u\frac{\partial \zeta}{\partial x} + \delta v\frac{\partial \zeta}{\partial y}}_{2' \text{ order}} + \zeta \underbrace{\left(\frac{\partial \delta u}{\partial x} + \frac{\partial \delta v}{\partial y}\right)}_{\mathrm{div}(\delta \vec{v})=0} \approx g\beta\frac{\partial \delta T}{\partial y}.$$

Consequently

$$\frac{\partial \zeta}{\partial t} \approx g\beta\frac{\partial \delta T}{\partial y}$$

$$\frac{\partial}{\partial t}\frac{\partial \delta T}{\partial y} = -\frac{\partial}{\partial y}\left[\delta u\left(\left.\frac{\partial \bar{T}}{\partial x}\right|_\infty + \frac{g}{C_p}\right)\right] \approx -\zeta\left(\left.\frac{\partial \bar{T}}{\partial x}\right|_\infty + \frac{g}{C_p}\right)$$

then by elimination of the variable $\delta T$:

$$\boxed{\ddot{\zeta} + g\beta\left(\left.\frac{\partial \bar{T}}{\partial x}\right|_\infty + \frac{g}{C_p}\right)\zeta = 0.} \quad (3b)$$

In this form, it is a pendulum oscillator which has always the same frequency as (4). It should be noted that this oscillation comes from a temperature disturbance, relations (3a), (3b), describe local reactions.

The oscillator period gives an oscillation time scale:

$$\boxed{t_{osc} = \frac{2\pi}{\sqrt{g\beta\left(\left.\frac{\partial \bar{T}}{\partial x}\right|_\infty + \frac{g}{C_p}\right)}}.} \quad (6)$$

With these results, the dimensionless parameter $gL/C_p(T_H - T_L)$ also appear.

### 4.2. Time scale analysis

As suggested by Bejan [6] p. 18, "The object of scale analysis is to use the basic principles of convective heat transfer in order to produce order of magnitude estimates for the quantities of interest". Turning now to the time scales used here:

#### 4.2.1. Boundary layer oscillation time.

Two possible situations are represented in Fig. 6. In mode (a), the instability comes from the plume which emerges at the top of the wall. Bejan in [6] p. 255 and [7] develops an analogy between the buckling of elastic solid columns and the meandering of inviscid stream. In mode (b), the instability comes from the travelling waves (of the Tollinien Schlichting type) in action in the boundary layer after a disturbance. In such a case, Bejan and Cunnington [16] propose a theoretical approach with an inviscid jet model. From [6] and [7], mode (a) leads to:

$$t_B \sim \frac{\lambda}{u_{av}}, \quad \frac{\lambda}{\delta} \sim \frac{\pi}{3^{1/2}} = 1.81$$

(for rectangular cross-section)

$$t_B = k_1\frac{\delta}{u_{av}} \quad \text{with } k_1 \sim 1.81.$$

In Fig. 1, $\lambda/\delta$ can be evaluated. It is distinctly superior to 1.81; consequently mode (a) is probably incorrect.

In mode (b) (evaluation from [16]), an inviscid jet next to the vertical wall is considered. The vorticity transport is explicated. Periodic solutions for disturbances are researched. As a result, some disturbances can be amplified if:

$$1.833 < \frac{\lambda}{\delta} < 4.701 \quad \text{with } 2.52\frac{\delta}{u_{av}} < t_B < 7.9\frac{\delta}{u_{av}}$$

i.e. here also $t_B = k_1(\delta/u_{av})$ but with $2.52 < k_1 < 7.9$.

In [14], an experimental study with water and uniform

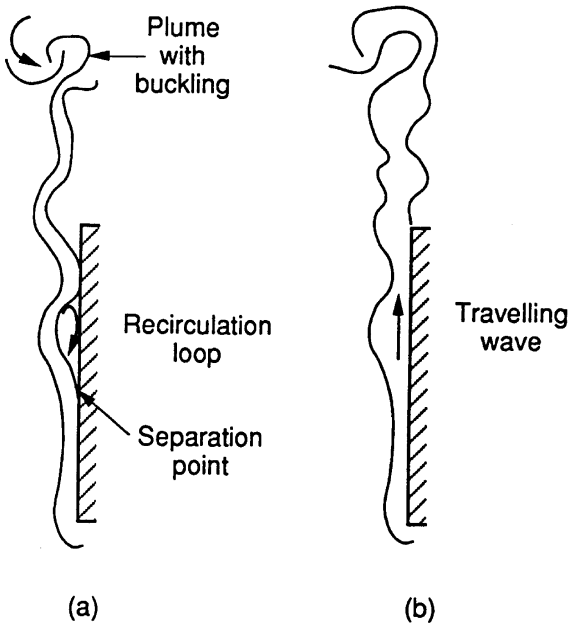


Fig. 6. Possible modes for boundary layer wave type.

flux on the wall gives: $180 < k_1 < 314$. The range for frequencies found is 0.08–6.35 Hz.

Other data is compiled in [15] and gives similar results.

#### 4.2.2. Transversal viscous communication time

It is the time taken for the viscous diffusion to penetrate sufficiently in the normal direction of the stream. In a first approximation, for a penetration of the order of $\delta$, it is:

$$t_v = k_2 \frac{\rho_\infty}{\mu_\infty}\delta^2 \quad \text{with } k_2 \sim 1/24.$$

For a penetration limited only to $\delta/3$ it would be:

$$k_2 \sim \frac{1}{3^2 \cdot 24} = 0.0046.$$

To evaluate time scales, take the velocity and the boundary layer thickness calculated by the integral method following once more the SQUIRE procedure (as reported in [29] p. 311), and ignore the $2^t$ order effects which arise from the vertical gradient of temperature outside the boundary layer.

$$\rho \frac{u_{av}x}{\mu} = \frac{5.17}{12}\left(\frac{20}{21}+Pr\right)^{-1/2} Gr_x^{1/2}$$

$$\frac{\delta}{x} = 3.93 Pr^{-1/2}\left(\frac{20}{21}+Pr\right)^{1/4} Gr_x^{-1/4}$$

where

$$Gr_x = g\beta(T_w - T_\infty)x^3\left(\frac{\rho}{\mu}\right)^2$$

finally

$$t_{osc} \approx \frac{2\pi}{\sqrt{g\beta\left(\left.\frac{\partial \overline{T}}{\partial x}\right|_\infty\right)}}$$

$$t_B \approx k_1 \frac{\delta}{u_{av}}$$

$$t_v \approx k_2 \frac{\rho_\infty}{\mu_\infty}\delta^2$$

from which follow the ratio:

$$\frac{t_v}{t_B} \approx \frac{\rho}{\mu}u_{av}\delta\frac{k_2}{k_1} = O(1)$$

$$\rightarrow \frac{5.17 \times 3.93}{12} Pr^{-1/2}\left(\frac{20}{21}+Pr\right)^{-1/4} Gr_x^{1/4}\frac{k_2}{k_1}$$

and with $Pr \sim 0.72$

$$\frac{t_v}{t_B} \approx 1.75\frac{k_2}{k_1} Gr_{x_{tr}}^{1/4} = O(1) \quad Gr_{x_{tr}} \rightarrow 0.105\left(\frac{k_1}{k_2}\right)^4 \tag{7}$$

with $Gr_{xtr} \sim 10^{14}$ as evaluated in Section 3, it gives:

if $k_2 \sim 1/24$ then $k_1 = 231$

if $k_2 \sim 0.0046$ then $k_1 = 25.7$.

Publications generally give $Gr_{xtr} > 4 \cdot 10^8$–$10^{10}$ depending on the author (see [14] Table 2 for air, the works of Griffiths and Davis, Saunders, Eckert and Soehgen, Harnett and Irvine, Warner, Cheesewright, Coutanceau). For the experiments grouped here with air and presurrized gas, transition occurs for $Gr_{xtr} > 10^8$–$10^{10}$, i.e. $149 < k_1/k_2 < 471$.

If this criterion had been correct, $k_1/k_2$ would be a constant but clearly it is not.

The experimental observations reported in Section 2 suggest evaluating $t_{osc}/t_B$ to check whether it is a constant. Physically, a constant value means that there is a coupling between the travelling waves and the Brunt–Väisälä oscillators. Reference [13] p. 273 gives some examples of coupled oscillators where each has a different frequency. There are many other examples of coupling with electrical circuits or mechanical oscillators.

In the present case, $t_{osc}/t_B$ has been evaluated by the same procedure as previously.

$$\frac{t_{osc}}{t_B} \approx \frac{2\pi}{\sqrt{g\beta\left(\left.\frac{\partial \overline{T}}{\partial x}\right|_\infty\right)}}\frac{U_{av}}{\delta k_1} = k_3$$

$$\frac{t_{osc}}{t_B} \approx \frac{2\pi}{k_1}\left(\frac{5.17}{12\times 3.93}\right)\left(\frac{20}{21}+Pr\right)^{-3/4}$$

$$\times Pr^{1/2} Gr_x^{1/4}\left(\frac{x}{(T_w - T_\infty)}\left.\frac{\partial \overline{T}}{\partial x}\right|_\infty\right)^{-1/2} = k_3$$

with $Pr \sim 0.72$

$$\frac{t_{osc}}{t_B} \approx \frac{0.3974}{k_1} Gr_x^{1/4}\left(\frac{x}{(T_w - T_\infty)}\left.\frac{\partial \overline{T}}{\partial x}\right|_\infty\right)^{-1/2} = k_3$$

$$\boxed{Gr_{x_{tr}} \rightarrow 40.1 k_1^4 k_3^4\left(\frac{x_{tr}\cdot\left.\frac{\partial T}{\partial x}\right|_{tr,\infty}}{T_w - T_\infty}\right)^2.} \tag{8}$$

The vertical gradient of temperature outside the boundary layer was not measured during the experiments except for the configuration of Fig. 9 relating to experiments

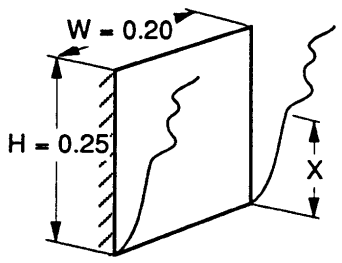


Fig. 7. Model put in a 0.7 m high pressurized vessel.

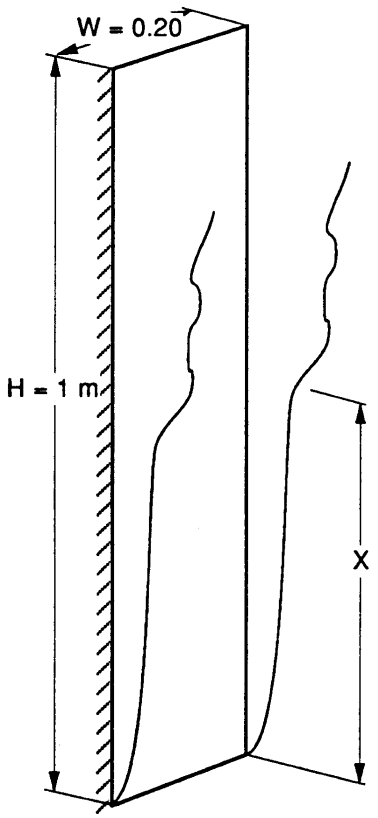


Fig. 8. Model put in the laboratory ambient conditions.

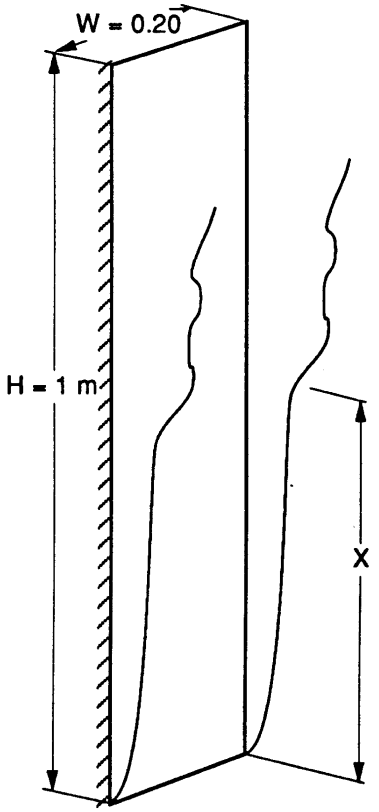


Fig. 9. Model put in a 1.6 m high pressurized vessel.

where a radiative emissivity of the wall is 0.51 instead of a very small value for the experiments given in Table 4. In this particular case (ref. [30]), the vertical gradient of temperature measured outside but near the boundary layer was:

$$\left.\frac{\partial T}{\partial x}\right|_{\infty} \sim 0.83 + \frac{T_w - T_\infty}{3}.$$

The constant part is the initial value before heating the wall. There are various possible explanations for the second part: first, it arises from the size of the closed pressurized vessel where the plane is placed, in which case it must be different for each configuration. Secondly, in the immediate neighbourhood of the boundary layer, it is a part of the hot fluid leaving the top of the wall which flows back after blending with the cold fluid to feed the boundary layer. Conduction also takes part in this process. In this case:

$$\left.\frac{\partial T}{\partial x}\right|_{\infty} \sim \left.\frac{\partial T}{\partial x}\right|_{\infty} \text{ before heating the wall} + \frac{T_w - T_\infty}{3H}$$

where $H$ is the height of the wall (1 m here).

This contribution would always be in a similar form for all the configurations.

—Another non-identified explanation.

Checking the second one with the various experiments, the results are plotted in Fig. 11. For each configuration there is a correlation in the form:

$$\frac{x_{tr}}{T_w - T_\infty}\left.\frac{\partial T}{\partial x}\right|_{\infty} = A \cdot Gr_{x_{tr}}^{1/2}.$$

It gives credit to the assumption that $t_{osc}/t_B = Cte$ as a good criterion for transition.

Coefficient $A$ would appear to depend on the size of the cavity containing the plane or on the height of the wall. This is perhaps only an appraisal of the conditions of observation of the transition which change with the size.

$A \sim 5 \cdot 10^{-6}$ for $H = 0.25$ m and a cavity of small size.
$A \sim 2.5 \cdot 10^{-6}$ for $H = 1$ m and a moderate sized cavity.
$A \sim 1.5 \cdot 10^{-6}$ for $H = 3.2$ m and a large space.

For what follows, $A \sim 5 \cdot 10^{-6}$ has been retained, this being the most restrictive, then:

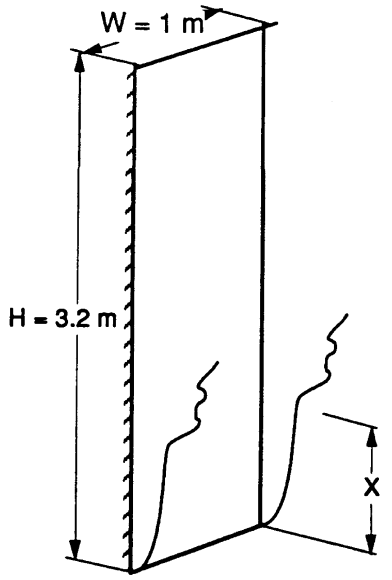


Fig. 10. Model put in ambient conditions in the 8.8 m high laboratory chamber (metallic silo for grain storage).

$k_1 k_3 \sim 178$.

The range of $t_{osc}$ during the experiments was:

$3\,s < t_{osc} < 30\,s$.

To reinforce these results, Fig. 12 shows a recording taken from [4]. There are electrical signals from a heat-flux meter placed on the wall and a thermocouple placed in the boundary layer, both at the same level $x$. There the convection is turbulent but the sensors are just beyond the transition.

The orders of magnitude of $t_{osc}$ and $t_B$ appear clearly: they are different. Moreover, according to the distance from the boundary layer, the vertical gradients of temperature can be different. It is possible that several Brunt–Väisälä oscillators can be activated, each having its own frequency.

Figure 13, from [31], gives recordings of the power spectral density for turbulence in free convection. They confirm the presence of very small frequencies.

To sum up, it is suggested that:

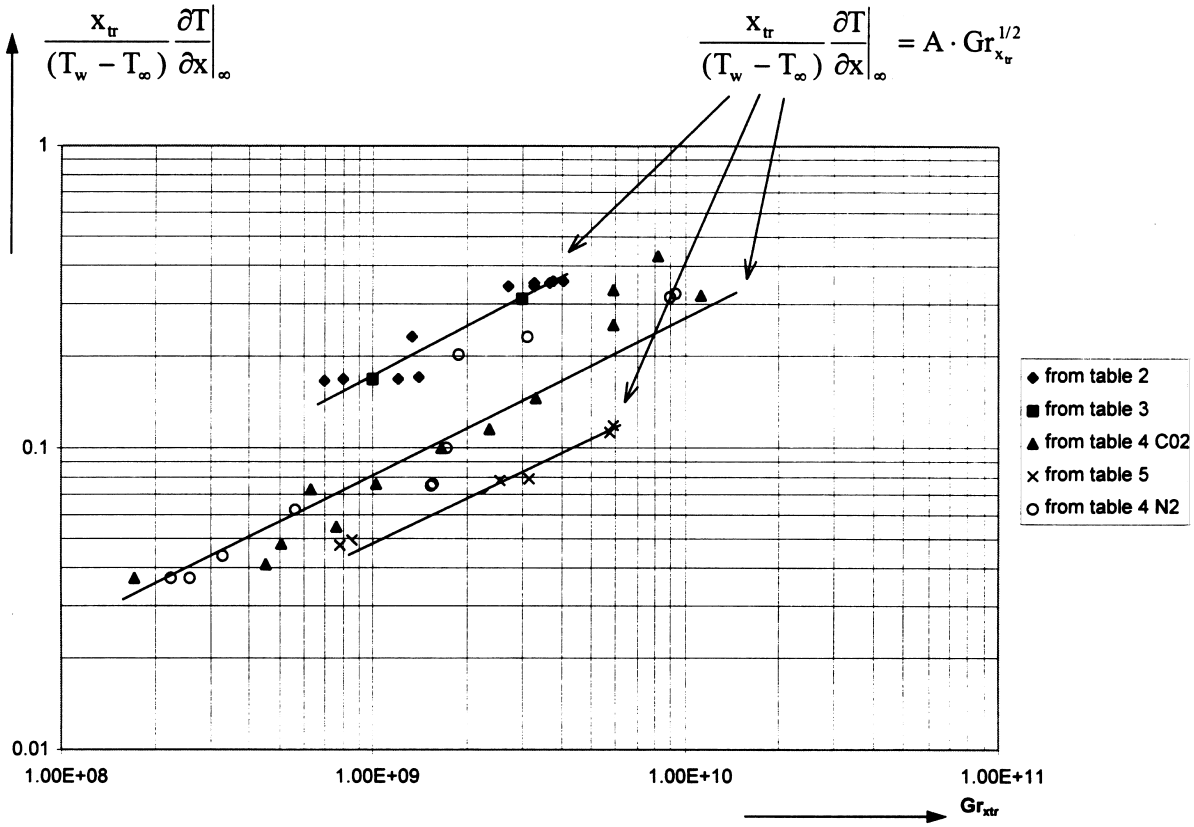


Fig. 11. Check of assumption $t_{osc}/t_B = Cte$.

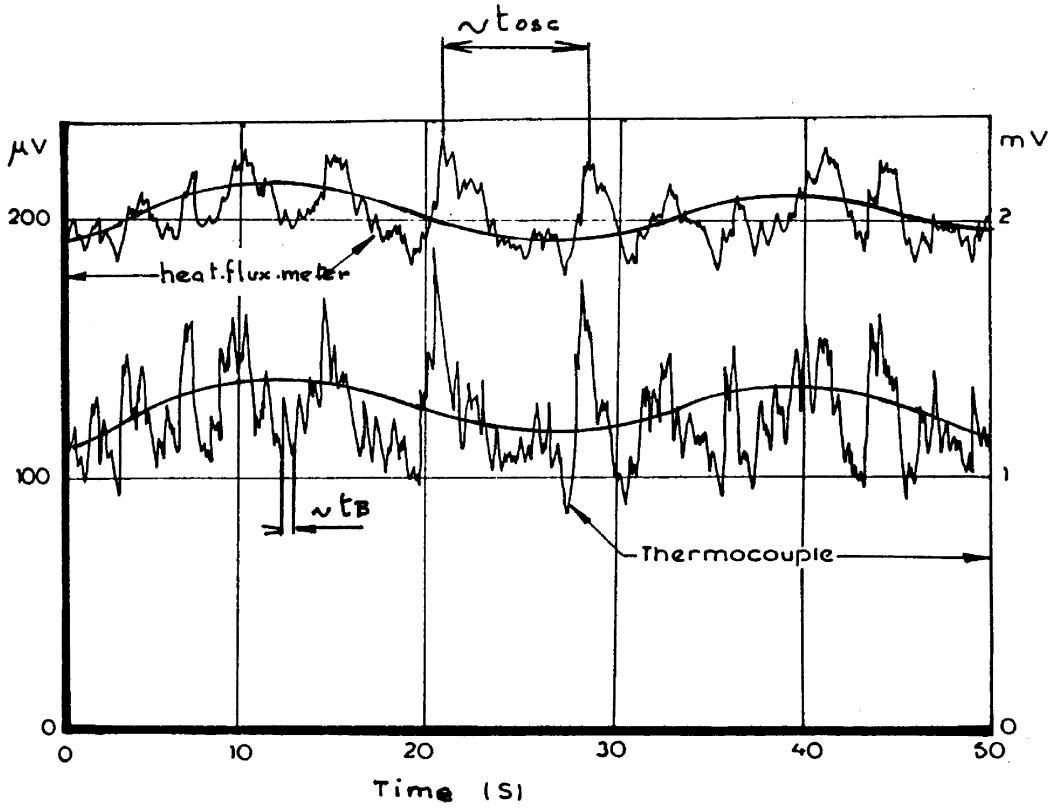


Fig. 12. From [4]. Simultaneous fluctuations of heatflux meter placed on the wall and fluid temperature in the boundary layer. $T_w = 153.3°C$; $y = 0.4$ mm; $x = 1.85$ m.

$$Gr_{x_{tr}}\left(\frac{T_w - T_\infty}{x_{tr}\cdot\left.\frac{\partial T}{\partial x}\right|_{tr,\infty}}\right)^2 = 4\cdot 10^{10}$$

$$\text{with}\left.\frac{\partial T}{\partial x}\right|_{tr,\infty} = \left.\frac{\partial T}{\partial x}\right|_{\text{before heating the wall}} + \frac{T_w - T_\infty}{3H}$$

be used henceforth as the condition for the onset of the transition to turbulence in free convection along an isothermal plane. The value of the constant and the vertical gradient of temperature are to be defined more exactly by new measurements.

## 5. Conclusions

Although it is widely conjectured that the onset of transition to turbulence in free convection along a flat vertical isotherm wall is conditioned by a constant Grashof number, this does not accord with experimental data.

Using the time scale analysis as Bejan does [6, 7], and by analogy with the Reynolds number in forced convection, it is shown, in stage one, that the ratio $t_v/t_B$ gives a transition condition of several orders of magnitude superior to the experimental data.

In stage two, a different approach is suggested to interpret the experimental transition condition. For this, a new time scale is introduced: outside the boundary layer there is a possible oscillation having a period $t_{osc}$ (new time scale equal to $2\pi/f_{BV}$).

The new time scale depends directly on the vertical gradient of temperature. The frequency $f_{BV}$ is distinctly lower than $f_B$, the frequency of the travelling waves. Consequently, a coupling type—not yet clearly explicated—must be involved in the process. In addition to the experimental observations, there are three factors in favour of coupling:

—linear and pendular modes of Brunt–Väisälä oscillator are possible in places near the boundary layer (local

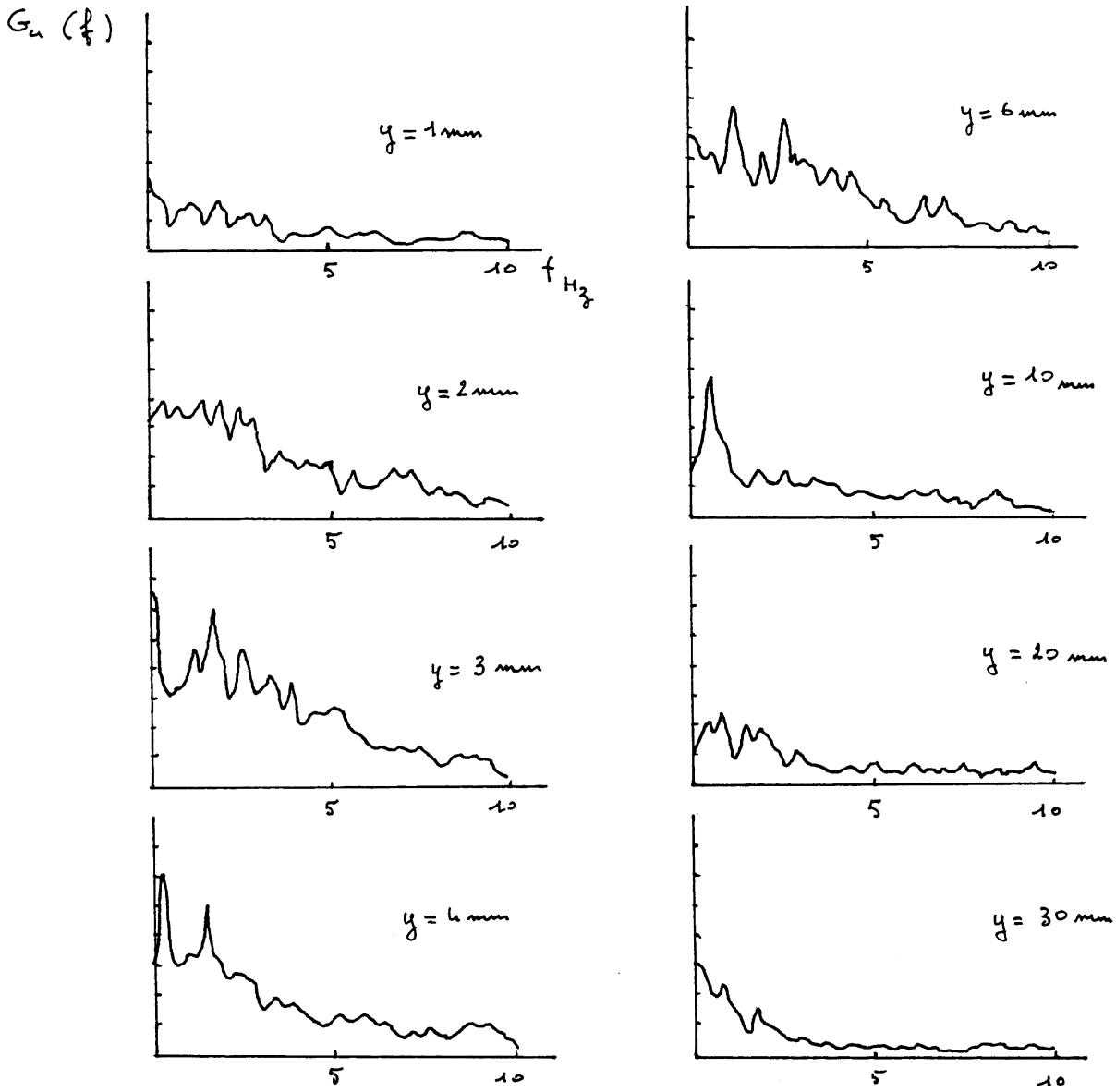


Fig. 13. (From [31].) Power spectral density. The configuration is as in Fig. 10. $x = 2.05$ m; $T_w = 100°C$. $G_u(f) = 4\int_0^\infty R_u(\tau)\cos 2\pi f\tau\,d\tau$ and $R_u(\tau) = \lim_{T\to\infty}\int_0^T u(t)u(t+\tau)\,dt$. $T$ = observation time.

oscillator). At the beginning of the transition the phenomenon is two-dimensional.

—locally, near the boundary layer, there can be a vertical gradient of temperature higher than farther away from the boundary layer.

—there is a domain of wavelengths where the travelling waves in the boundary layer are amplified.

The oscillator reacts to oscillations coming from the traveling waves and provokes the onset of transition to turbulence. The measurements show that this occurs in normal conditions before the viscous dissipation becomes insufficient to dampen the travelling waves.

In the final stage, a check is carried out that all is in accordance with the experimental data. In the immediate neighbourhood of the boundary layer, the vertical gradient of temperature is affected by a partial recirculation in the stream leaving the top of the wall. It is in this area that the Brunt–Väisälä oscillation is activated.

Natural convection in vertical configurations is a good

example to study the two-dimensional transition to turbulence. Locally at co-ordinate $x$, there are the degrees of freedom : $\delta$, $u$, and the interaction with an outer oscillator, to give rise to chaos.

A similar analysis should be possible to determine the condition for transition in vertical cells, but the problem is more complex because there are several means of steady flows according to values for the Grashof number and the aspect ratio height/width. The waves are also probably affected by the width of the cells. It is an interesting challenge for future research. For this purpose, experimental data is available (e.g. ref. [5] with rectangular cells of large aspect factor H/W and filled with pressurized gas). Techniques for numerical simulations also exist (e.g. [24, 26–28]).

A specially designed user-friendly method of visualisation in natural convection is proposed in ref. [32]. Particular attention would be paid to the vertical temperature gradient.

**Acknowledgement**

The authors wish to express their gratitude to Nan Miller for her help with the translation of their publication.

**Appendix**

Data from [1]. $P_0 = 1$ atm. Data from [2] (extracts only, other data corresponding to tests for an eventual radiating effect). $P_0 = 1$ atm. Data from [4], $P_0 = 1$ atm. Transition observed by heat flux meter placed on the plane.

Table A1
Different sizes of the plane and the surrounding conditions

| Ref. | Flat size | | Surrounding |
|---|---|---|---|
| | $H$ (m) | $W$ (m) | |
| $[1]_a$ | 0.25 | 0.2 | $CO_2$ pressurized vessel of low height (0.7 m) |
| $[1]_b$ | 1 | 0.2 | Air in ambient conditions and with plane placed in a basement approximately 1.9 m high |
| [2] | 1 | 0.2 | 1.6 m high $CO_2$ pressurized vessel |
| | 1 | 0.2 | 1.6 m high $N_2$ pressurized vessel |
| [4] | 3.2 | 1 | Air in ambient conditions. Model put in a large silo for grain storage (metallic walls) |

Table A2
$CO_2$ in pressurized vessel of low height (see Fig. 7)

| Fluid | $P/P_0$ | $(T_w - T_\infty)$ (K) | $x$ (m) | $Gr_x \cdot 10^{-8}$ |
|---|---|---|---|---|
| $CO_2$ | 4 | 32.6 | 0.25 | 27 |
| | 4 | 95.5 | 0.125 | 7 |
| | 5 | 24 | 0.25 | 33 |
| | 5 | 25.4 | 0.17 | 13.4 |
| | 5 | 52 | 0.125 | 8 |
| | 6 | 14.7 | 0.25 | 33 |
| | 7 | 12 | 0.25 | 37 |
| | 7 | 33 | 0.125 | 12 |
| | 8 | 9.9 | 0.25 | 41 |
| | 9 | 7 | 0.25 | 38 |
| | 9 | 23.2 | 0.125 | 14 |

Table A3
Air in ambient conditions (see Fig. 8)

| Fluid | $P/P_0$ | $(T_w - T_\infty)$ (K) | $x$ (m) | $Gr_x \cdot 10^{-8}$ |
|---|---|---|---|---|
| Air | 1 | 68 | 0.90 | 30 |
| | 1 | 130 | 0.50 | 10 |

Table A4
$CO_2$ and $N_2$ in pressurized vessel of medium height (see Fig. 9)

| Fluid | $P/P_0$ | $(T_w - T_\infty)$ (K) | $T_w$ (K) | $x$ (m) | $Gr_x \cdot 10^{-8}$ |
|---|---|---|---|---|---|
| $CO_2$ | 2 | 11 | 298 | 0.78 | 113.1 |
| | 2 | 11.7 | 302.5 | 0.63 | 59.1 |
| | 2 | 63.8 | 369.5 | 0.21 | 6.28 |
| | 3 | 3.5 | 288.4 | 0.75 | 81.6 |
| | 3 | 4.3 | 289.9 | 0.63 | 58.9 |
| | 3 | 28.6 | 322 | 0.21 | 10.2 |
| | 3 | 50.2 | 349.2 | 0.105 | 1.72 |
| | 7 | 5.9 | 294 | 0.21 | 16.6 |
| | 7 | 14.5 | 305 | 0.105 | 4.51 |
| | 10 | 3.8 | 292.2 | 0.21 | 23.7 |
| | 10 | 6.8 | 296 | 0.105 | 5.08 |
| | 14 | 2.3 | 288.3 | 0.21 | 33.4 |
| | 14 | 4.4 | 291.2 | 0.105 | 7.66 |
| $N_2$ | 2 | 15.3 | 302.2 | 0.73 | 29.8 |
| | 2 | 25.5 | 316.6 | 0.63 | 31.2 |
| | 7 | 4.7 | 288.8 | 0.63 | 93.0 |
| | 7 | 4.9 | 293.7 | 0.63 | 89.8 |
| | 7 | 28.9 | 321.0 | 0.21 | 15.5 |
| | 7 | 31.8 | 332.5 | 0.21 | 15.4 |
| | 7 | 50.8 | 350.5 | 0.105 | 2.6 |
| | 7 | 47.5 | 354.4 | 0.105 | 2.26 |
| | 14 | 5.9 | 290.0 | 0.21 | 17.3 |
| | 14 | 9.8 | 297.2 | 0.105 | 3.30 |
| | 30 | 1.3 | 284.0 | 0.21 | 18.9 |
| | 30 | 3.2 | 286.7 | 0.105 | 5.65 |

Table A5
Air in ambient conditions (see Fig. 10)

| Fluid | $P/P_0$ | $(T_w - T_\infty)$ (K) | $T_w$ (K) | $x$ (m) | $Gr_x \cdot 10^{-8}$ |
|---|---|---|---|---|---|
| Air | 1 | 52.9 | 335 | 0.98 | 59.2 |
| | 1 | 71.9 | 367 | 0.97 | 57.1 |
| | 1 | 108.1 | 391 | 0.71 | 31.7 |
| | 1 | 110.4 | 407 | 0.70 | 25.6 |
| | 1 | 152.6 | 433 | 0.43 | 7.83 |
| | 1 | 153.3 | 438 | 0.45 | 8.53 |

## References


[1] Mordchelles-Regnier G, Kaplan C. Visualization of natural convection on a plane wall and in a vertical gap by differential interferometry—transition and turbulent regime. Proceedings of the 1963 Heat Transfer and Fluid Mechanics Institute. Stanford University Press, 1963.

[2] Jannot M, Morchelles-Regnier G, Terpstra J. Critère de stabilité d'une couche limite de convection naturelle sur une paroi plane verticale et isotherme. CR Acad Sc Paris, serie A 1968;267:617–20.

[3] Jannot M, Terpstra J, Viannay S. Critère de stabilité d'une couche limite de convection naturelle sur une paroi plane verticale isotherme ou soumise à une répartition linéaire de température. CR Acad Sc Paris, serie B 1970;271:177–9.

[4] Pirovano A, Viannay S, Jannot M. Convection naturelle en régime turbulent le long d'une plaque plane verticale. Euratom report EUR 4489 f, Luxembourg, July 1970.

[5] Jannot M, Mazeas C. Etude expérimentale de la convection naturelle dans des cellules rectangulaires verticales. Int J Heat Mass Transfer 1973;16:81–100.

[6] Bejan A. Convection Heat Transfer. 2nd ed. New York : John Wiley and Sons, 1995.

[7] Bejan A. Buckling flows. A new frontier in fluid mechanics. Annual Review of Numerical Fluid Mechanics and Heat Transfer. Washington, DC : 1987;1:262–304.

[8] Gebhart B, Jaluria Y, Mahajan RL, Sammakia B. Buoyancy induced flows and transport. New York : Hemisphere, 1988.

[9] Glansdorff P, Prigogine I. Structure stabilité et fluctuations. Paris : Masson, 1971. p. 178.

[10] Berge P, Pommeau Y, Vidal C. L'ordre dans le chaos. Vers une approche déterministe de la turbulence. Paris : Hermann, 1984. p. 92.

[11] Strogatz SH. Non-linear Dynamics and Chaos. New York : Addison Wesley, 1994. p. 273.

[12] Lorentz EN. Deterministic non-periodic flow. J Atmos Sci 1963;20:130.

[13] Dring R, Gebhart B. A theoretical investigation of disturbance amplification in external laminar natural convection. J Fluid Mech 1968;34:551–64.

[14] Godaux F, Gebhart B. An experimental study of the transition of natural convection flow adjacent to a vertical surface. Int J Heat Mass Transfer 1974;17:93–107.

[15] Gebhart B, Mahajan R. Characteristic disturbance frequency in vertical natural convection. Int J Heat Mass Transfer 1975;18:1143–8.

[16] Bejan A, Cunnington GR. Theoretical considerations of transition to turbulence in natural convection near a vertical wall. Int J Heat and Flow 1983;4(3):131–9.

[17] Väisälä V. Uber die Wirkung der Windschwankungen auf die Pilot-Beobachtungen. Soc Scient Fennica, Commentat Phys Maths 1925;2:38–46.

[18] Brunt D. The period of simple vertical oscillations in the atmosphere. Quarterly Journal of Royal Meteorological Society 1927;53:30–2.

[19] Thorpe SA. On standing internal gravity waves of finite amplitude. J Fluid Mech 1968;32(3):489–528.

[20] Benielli D. Excitation paramétrique et déferlement d'ondes internes en fluide stratifié. Thèse de doctorat no. 62, Université Claude Bernard Lyon 1, 1995.

[21] Benielli D, Sommeria J. Excitation of internal waves and stratified turbulence by parametric instability. Dynamics of Atmospheres and Oceans 1996;23:335–43.

[22] Ndame A. Etude expérimentale de la convection naturelle en cavité. De l'état stationnaire au chaos. Thèse de doctorat, Université de Poitiers, juin, 1992.

[23] Penot F, Ndame A. Successive bifurcations of natural convection in a vertical enclosure heated from the side. Institution of Chemical Engineers Symposium Series, 1992;1:139, 507–13.

[24] Xin S, Le Quéré P. Direct numerical simulation of two-dimensional chaotic natural convection in a differentially heated cavity of aspect ratio 4. J Fluid Mech 1995;304:87–118.

[25] Patterson JC, Imberger J. Unsteady natural convection in a rectangular cavity. J Fluid Mech 1980;100(1):65–86.

[26] Le Quéré P. Transition to chaos in cavity heated from the side. Institution of Chemical Engineers Symposium Series 1992;2:129, 1267–82.

[27] Le Quéré P. Onset of unsteadiness, routes to chaos and simulations of chaos flows in cavities heated from the side : a review of present status. Heat Transfer, Proc 10th Int Heat Transfer Conf Brighton, U.K., 1994;1:281–96.

[28] Henkes RAWM, Le Quéré P. Three-dimensional transition of natural convection flows. J Fluid Mech 1996;319:281–303.

[29] Eckert ERG, Drake RM Jr. Heat and Mass Transfer, 2nd ed. New York : McGraw-Hill, 1959.

[30] Jannot M. Convection naturelle le long d'une plane verticale. Détermination des critères de transition à la turbulence. Contrat Euratom 063-64 TEGF, 1964.

[31] Delisee A, Jannot M, Locatelli G. Modélisation pour le calcul d'écoulements turbulents en convection naturelle. Marché DGRST 72-7-089500-75-01. Collaboration entre BERTIN et Cie et le Laboratoire de Mécanique expérimentale des fluides. Université Paris VI Orsay.

[32] Grossin R, Jannot M, Viannay S. Schlieren visualization device allowing an arbitrary orientation of the lines with respect to the scanning direction. Applied Optics 1971;10:201.